Spectroscopy of ^{98}Cd by two-nucleon removal from ^{100}In

S. Y. Jin[1,3,4], S. T. Wang[1,3],* J. Lee[2],† A. Corsi[5], K. Wimmer[6], F. Browne[7], S. Chen[2], M. L. Cortés[8], P. Doornenbal[7], T. Koiwai[9,7], C. X. Yuan[10], A. Algora[11,12], D. Brugnara[8,13], J. Cederkäll[14], J. Gerl[15], M. Górska[15], G. Häfner[16,17], K. Kokubun[9], P. Koseoglou[18,15], S. Kubono[7], P. Li[2], P. Liang[2], J. Liu[1,2], Z. Liu[1,3], T. Lokotko[2], J. Park[19], H. Sakurai[7,9], L. G. Sarmiento[14], Z. Y. Sun[1,3], R. Taniuchi[7,20], W. Xian[2], and I. Zanon[8]

1 CAS Key Laboratory of High Precision Nuclear Spectroscopy, Institute of Modern Physics,
Chinese Academy of Sciences, Lanzhou 730000, China
2 Department of Physics, The University of Hong Kong, Pokfulam, 999077, Hong Kong, China
3 School of Nuclear Science and Technology, University of Chinese Academy of Sciences, Beijing 100049, China
4 School of Nuclear Science and Technology, Lanzhou University, Lanzhou 730000, China
5 IRFU, CEA, Université Paris-Saclay, 91191 Gif-sur-Yvette, France
6 Instituto de Estructura de la Materia, CSIC, E-28006 Madrid, Spain
7 RIKEN Nishina Center, Wako, Saitama 351-0198, Japan
8 Istituto Nazionale di Fisica Nucleare, Laboratori Nazionali di Legnaro, I-35020 Legnaro, Italy
9 Department of Physics, University of Tokyo, 7-3-1 Hongo, Bunkyo, Tokyo 113-0033, Japan
10 Sino-French Institute of Nuclear Engineering and Technology,Sun Yat-Sen University, Zhuhai, 519082, Guangdong, China
11 IFIC, CSIC-University of Valencia, Valencia, Spain
12 Institute of Nuclear Research (ATOMKI), Debrecen, Hungary
13 Dipartimento di Fisica e Astronomia Università di Padova and INFN, I-35131 Padova, Italy
14 Department of Physics, Lund University, S-22100 Lund, Sweden
15 GSI Helmholtzzentrum für Schwerionenforschung GmbH, 64291 Darmstadt, Germany
16 Université Paris-Saclay, CNRS/IN2P3, IJCLab, 91405 Orsay, France
17 Institut für Kernphysik, Universität zu Köln, 50937 Köln, Germany
18 Institut für Kernphysik, Technische Universität Darmstadt, 64289 Darmstadt, Germany
19 Center for Exotic Nuclear Studies, Institute for Basic Science, 34126 Daejeon, Korea
20 Department of Physics, University of York, Heslington, York YO10 5DD, United Kingdom

(Dated: June 25, 2021)

Low-lying states of ^{98}Cd have been populated by the two-nucleon removal reaction (^{100}In,^{98}Cd+γ) and studied using in-beam γ-ray spectroscopy at the Radioactive Isotope Beam Factory at RIKEN. Two new γ transitions were identified and assigned as decays from a previously unknown state. This state is suggested to be based on a $\pi 1g_{9/2}^{-1} 2p_{1/2}^{-1}$ configuration with $J^\pi = 5^-$. The present observation extends the systematics of the excitation energies of the first 5^- state in $N = 50$ isotones toward ^{100}Sn. The determined energy of the 5^- state in ^{98}Cd continues a smooth trend along the $N = 50$ isotones. The systematics are compared to shell-model calculations in different model spaces. Good agreement is achieved when considering a model space consisting of the $\pi(1f_{5/2}, 2p_{3/2}, 2p_{1/2}, 1g_{9/2})$ orbitals. The calculations with a smaller model space omitting the orbitals below the $Z = 38$ subshell could not reproduce the experimental energy difference between the ground and first 5^- states in $N = 50$ isotones, because proton excitations across $Z = 38$ subshell yield a large amount of correlation energy that lowers the ground states.

I. INTRODUCTION

The nuclear structure of the self-conjugate doubly-magic ^{100}Sn and its neighboring nuclei has been the subject of intense experimental and theoretical interest, since it provides a unique testing ground for the nuclear shell model and is important for the astrophysical rapid-proton capture process [1]. However, nuclei in the vicinity of ^{100}Sn lie well away from the stability line and experimental investigations of their spectroscopic properties are still limited. In particular, experimental information on excited states of ^{100}Sn is yet to be obtained, where the excited state energies would provide impor-

tant information on the $N = Z = 50$ shell gap and a direct benchmark to the development of structure models around the $A \sim 100$ proton-rich nuclei region. Experimental information from the neighboring nuclei is indispensable in understanding the nuclear structure of this region and could serve as a stepping stone toward ^{100}Sn. In the ^{100}Sn region, the evolution of the $0_{\rm gs}^+ \rightarrow 2_1^+$ transition strengths in light $Z = 50$ isotopes toward ^{100}Sn has been the subject of continued experimental and theoretical efforts [2–8]. The neutron-proton interaction in $N = Z$ nuclei below ^{100}Sn has become an attractive research topic in recent years [9–14]. For example, recent experimental work on the level structure of ^{92}Pd [9] and ^{96}Cd [11] has revealed the importance of the isoscalar neutron-proton interaction for self-conjugate nuclei close to ^{100}Sn. The proton-rich $N = 50$ isotones below ^{100}Sn have also attracted considerable interest [15–29], where

---

highlights include the discovery of seniority isomers [17] and $N = 50$ core excited states [19–22].

The nucleus ^{98}Cd ($Z = 48$, $N = 50$), two proton holes from ^{100}Sn, is so far the most proton-rich $N = 50$ isotone for which information about excited states is available [15–19]. In previous studies on ^{98}Cd, its excited states have been populated via isomer-delayed γ-ray spectroscopy following fusion-evaporation reactions [17–19] and fragmentation reactions [15, 16]. The $\pi 1 g_{9/2}^{-2}$ seniority $\nu = 2$ states with $J^\pi = (2^+)$, (4^+), (6^+), and (8^+); and two core-excited states of (10^+) and (12^+) [18, 19], based on the $(\pi 1 g_{9/2}^{-2})(\nu 1 g_{9/2}^{-1} 2 d_{5/2}^1)$ configuration, have been observed. In a conference report [30], it is mentioned that the level scheme of ^{98}Cd is extended tentatively to 15^+ by using a fusion-evaporation reaction, but no details are presented. Various shell model calculations [17, 31–33] have been performed to study the structure of ^{98}Cd, and some low-lying states associated with the single-particle excitations from the proton $\pi 2 p_{1/2}$ or $\pi 2 p_{3/2}$ to $\pi 1 g_{9/2}$ orbitals are predicted. However, none of these states have been identified experimentally in previous studies because these states are not populated in the decay of the known isomers and are also difficult to investigate using in-beam γ-ray spectroscopy following fusion-evaporation reactions due to their non-yrast nature. It is noted that in the neighboring even-A ^{100,102}Cd isotopes, these single-particle states are also not observed, although a large number of high-spin states have been established in ^{100,102}Cd via fusion-evaporation reactions. Nucleon-removal reactions in inverse kinematics at intermediate energies are a valuable tool to populate single-particle states, and thus reactions involving proton removal can be used as a complementary method to probe the proton single-particle structure of these neutron-deficient Cd isotopes.

In the present work, we report on an in-beam γ-ray spectroscopy study on ^{98}Cd populated in the two-nucleon removal reaction from a ^{100}In secondary beam, in order to extend the spectroscopic information of ^{98}Cd and enhance the understanding of its structure in the context of the doubly magic ^{100}Sn region.

II. EXPERIMENTAL PROCEDURE

The present experiment was carried out at the Radioactive Isotope Beam Factory (RIBF), operated by the RIKEN Nishina Center and the Center for Nuclear Study of the University of Tokyo. A ^{124}Xe primary beam was accelerated to 345 MeV/nucleon and impinged on a 5-mm-thick ^{9}Be production target placed at the entrance of the BigRIPS fragment separator [34]. The radioactive cocktail beams of interest, including ^{100}In, were separated and identified in BigRIPS event by event based on the measurements of time-of-flight (TOF), magnetic rigidity ($B\rho$), and energy loss (ΔE) [35], and transported to the reaction target location in front of the ZeroDegree spectrometer.

The secondary ^{100}In beam then impinged on the reaction target with an energy of $\sim$175 MeV/nucleon in front of the target to produce the two-nucleon removal residues ^{98}Cd. The reaction residues were identified in the ZeroDegree spectrometer following a similar method as for BigRIPS. Two reaction target settings were used during this experiment, employing a 5-mm-thick CH_2 target and a 3-mm-thick C target.

Prompt γ rays emitted from excited states of ^{98}Cd were detected with the upgraded DALI2$^+$ array [36, 37] surrounding the reaction target. DALI2$^+$ consisted of 226 NaI(Tl) detectors, covering center-of-crystal polar angles in the range from 16° to 123°. Energy calibrations were performed using ^{88}Y, ^{60}Co and ^{137}Cs sources. Emitted γ rays from the fast moving nuclei experienced a large Doppler shift, and therefore the γ-ray spectra were corrected based on the individual detector angles and the reaction-product velocities. In the analysis, an energy add-back procedure was applied for hits detected within 15 cm radius to increase the photopeak efficiency.

III. RESULTS

The Doppler-corrected γ-ray spectrum of the $CH_2(^{100}$In, ^{98}Cd$+\gamma)$ reaction is displayed in Fig. 1. A similar result is obtained for the C target setting. In Fig. 1(a) no cut on the γ-ray detection multiplicity, M_γ, was applied. The spectra for $M_\gamma = 1$, 2 and 3 events are shown in Fig. 1(b).

As can be seen in Fig. 1(a), four peaks are clearly visible, of which the two peaks at lower energies are observed in the present experiment for the first time. The two strong peaks at higher energies are suggested to correspond to the previously observed 688-keV ($4^+ \rightarrow 2^+$)
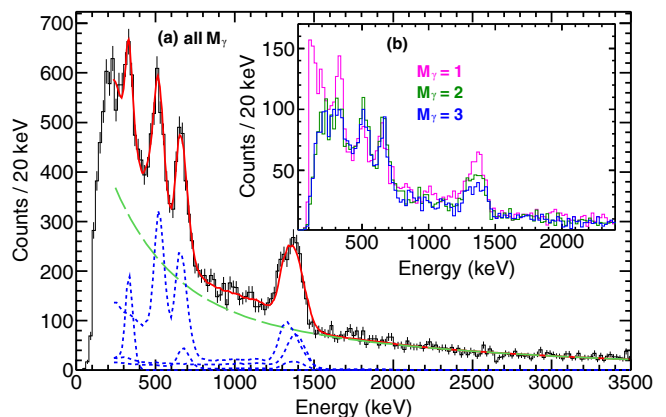

FIG. 1. (a) Doppler-corrected γ-ray energy spectrum of ^{98}Cd following the $CH_2(^{100}$In, ^{98}Cd) reaction with no γ-ray multiplicity restrictions. The fit function to the spectrum (red solid line) includes simulated response functions for the single and cascade transitions (blue dotted lines) and a double-exponential background (green dashed line). The inset (b) shows the spectra for $M_\gamma = 1$, 2 and 3.
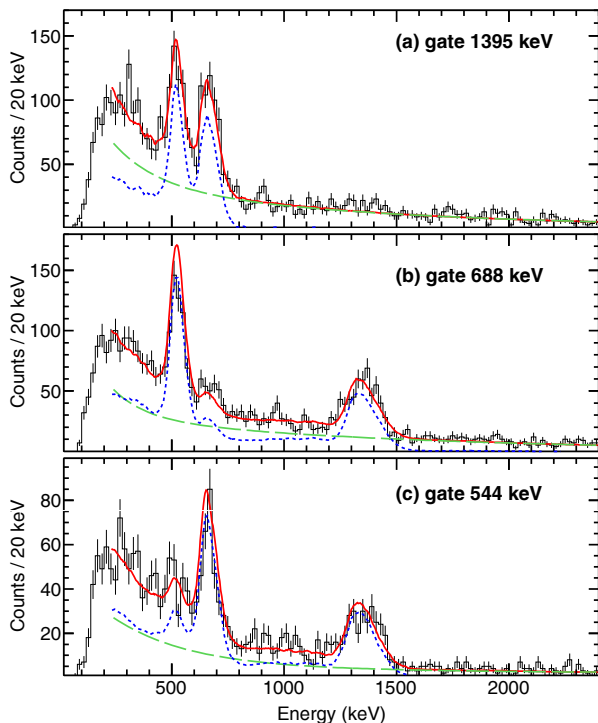
FIG. 2. γ-γ coincidence spectra. Panels (a), (b), and (c) show the spectra gated on the 1395-, 688-, and 544-keV transitions, respectively. The blue dotted lines show simulated response functions for the number of expected coincidences based on the proposed level scheme in Fig. 3 and the direct population intensity determined from the fitting shown in Fig. 1. A double-exponential background (green dashed line) is coupled to the simulated response function in order to get the fit function (red solid line) to the gated spectrum.

and 1395-keV $(2^+ \rightarrow 0^+)$ transitions, respectively. An energy shift of these two peaks compared to actual values is observed. The shift can be explained as due to the influence of lifetimes of the decaying excited states. Excited-state half-lives with tens of ps or longer will shift peaks to lower Doppler-reconstructed energies as compared to their actual values. After taking into account the excited state lifetime effects, the newly observed transitions are determined to be 346(8) and 544(12) keV by fitting the spectrum in Fig. 1(a) with simulated DALI2$^+$ response functions (see below).

To establish the level scheme for the new transitions observed in the singles spectrum, γ-γ coincidence spectra are produced and shown in Fig. 2. The obtained spectra for the CH$_2$ and C target are essentially the same and therefore are combined in the γ-γ coincidence analysis. The level scheme of ^{98}Cd, displayed in Fig. 3, is constructed based on the γ-γ coincidence relationships in combination with previously known information [15, 17–19]. As can be seen in Fig. 2, the newly observed 544(12)-keV transition has a clear coincidence with the previously known transitions at 688 keV [$(4^+) \rightarrow (2^+)$] and 1395 keV [$(2^+) \rightarrow 0^+$], and thus forms a cascade with the

$(4^+) \rightarrow (2^+)$ and $(2^+) \rightarrow 0^+$ transitions, suggesting that this new γ ray feeds the known (4^+) state at 2083 keV. Therefore, the 544(12)-keV transition is placed as decaying from a new state at 2627(12) keV to the (4^+) state, as shown in Fig. 3.

As illustrated in Fig. 1(b), the γ-ray spectrum for γ-ray multiplicity M$_\gamma$ = 1 displays a strong peak at 346(8) keV, while in the spectra for M$_\gamma$ = 2 and 3 the position at 346(8) keV does not show a strong peak as compared to the neighboring 544(12)- and 688-keV transitions. Furthermore, the γ-γ coincidence analysis indicates that none of the other transitions is seen in coincidence with the 346(8)-keV transition, suggesting that this transition should feed the ground state or an isomeric state. The possibility for the 346(8)-keV transition to be a direct ground state decay from a state at 346(8) keV can be excluded. Such a state would lie far below the first 2^+ state at 1395 keV, which is not expected for the semi-magic ^{98}Cd. Therefore, the 346(8)-keV transition most likely populates an isomeric state. The possibility for this transition to feed the known 154(16)-ns (8^+)isomer at 2428 keV can not be ruled out based on the present experiment, but it can be discarded by comparison to the shell model calculations as described below and shown in Fig. 3. The 346(8)-keV transition is in agreement with the energy difference between the newly identified 2627(12)-keV state and the previously observed 13(2)-ns isomeric (6^+) state at 2281 keV, thus is tentatively placed as feeding the (6^+) isomer from the 2627(12)-keV level.

The singles spectrum in Fig. 1(a) is fitted with simulated DALI2$^+$ response functions based on GEANT4 framework [38, 39] added on a double-exponential background. In the simulations, the precise energies of the 1395- and 688-keV transitions determined previously are employed when obtaining the DALI2$^+$ response functions. The half-lives for each excited state are considered in the simulations. The (6^+) state in ^{98}Cd, as shown in Fig. 3, is known to have a half-life of $T_{1/2} = 13(2)$ ns [15], while the half-lives of the (2^+) and (4^+) states are experimentally unknown. For the (2^+) and (4^+) states, the deduced half-lives from the calculated $B(E2)$ values using different shell models are very similar. In Ref. [26], the half-life of the (2^+) state is expected to be below 1 ps based on the calculated $B(E2)$ values from all three models and the (4^+) state half-life is expected to be in the range of $17 - 30$ ps. The (2^+) state half-life is assumed to be 0 ps in the simulations, since ~ 1 ps uncertainty in the half-life leads to negligible effect on the deduced γ-ray energy. Considering that the SDGN model predictions [26] provide better agreement with the experimentally known $(4^+) \rightarrow (2^+)$ transition strength for the neighboring $N =$ 50 isotones ^{96}Pd and ^{94}Ru, the SDGN model predicted half-life of 17 ps for the (4^+) state of ^{98}Cd is taken as input for the simulations.

In addition to keeping the half-lives of the (2^+) $(T_{1/2} = 0$ ps), (4^+) ($T_{1/2} = 17$ ps), and (6^+) ($T_{1/2} = 13$ ns) states and the energies of the 1395- and 688-keV transitions fixed, the half-life and energy of the newly observed
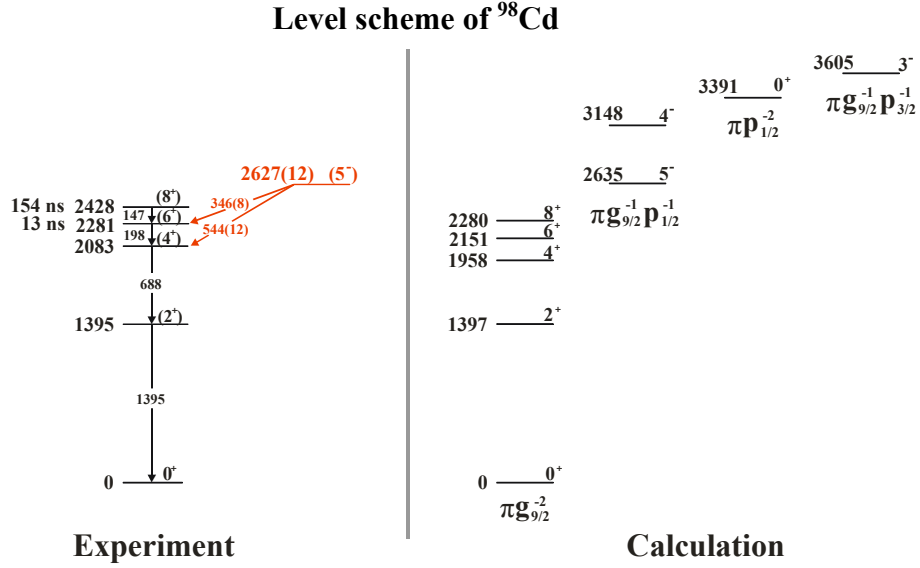
Level scheme of ^{98}Cd

FIG. 3. Level schemes of ^{98}Cd constructed experimentally and predicted by shell model calculations. The transitions and the level energies are in keV. The red level and transitions are established from the present experiment.

state are treated as free parameters in the simulations. It is found that a half-life of 100(30) ps and an energy of 2627(12)keV for the newly identified state can best describe the experimental spectrum by considering the response functions for the following single and cascade γ transitions: (a) a 1395-keV γ ray emitted following the direct population of the (2^+) state in the reaction, (b) a cascade of two γ rays (688 keV $\rightarrow$ 1395 keV) emitted following the population of the (4^+) state, (c) a cascade of three γ rays [544(12) keV $\rightarrow$ 688 keV $\rightarrow$ 1395 keV] emitted following the population of the 2627(12)-keV state, and (d) a 346(8)-keV transition emitted from the decay of the 2627(12)-keV state to the (6^+) isomeric state.

Based on the simulations, the populated intensities for the detected γ rays and excited states are extracted. The relative intensities of the γ rays at 1395, 688, 544(12), and 346(8) keV are deduced to be 100(12)%, 63(7)%, 54(3)%, and 26(3)%, respectively. The direct populations of each excited state are deduced to be 100(8)%, 12(5)%, and 46(6)%, for 2627(12), 2083, and 1395 keV, respectively. The proposed level scheme and the determined direct population intensities for each excited state are employed to get simulated response functions for the number of expected coincidences in the gated spectra, as shown by blue dotted lines in Fig. 2. To have a better comparison to the experimental spectrum, a double-exponential background is added to the simulated response function. It can be been in Fig. 2 that the simulated spectra (red solid lines) are in overall good agreement with the experimental results. It is noted that self-coincidence is observed in the coincidence spectra gated on 544- and 688-keV transitions. The self-coincidence originates from the contributions to the energy gate from the Compton background of the 1395-keV transition. The gate on the 1395-keV transition, in contrast, is much cleaner because

of the lower background at higher energies and the fact that no γ rays are observed above 1395 keV.

IV. DISCUSSION

As shown in Fig. 3, the newly identified 2627(12)-keV state decays to the (4^+) and (6^+) states. The decay pattern of the 2627(12)-keV state suggests that the possible spin-parity for this state could be 4^+, 5^+, 6^+ or 5^-. To further probe the nature of the 2627(12)-keV state, shell-model calculations have been performed using the KSHELL code [40] with the modified jj45pna Hamiltonian. The jj45pna Hamiltonian is derived from the CD-Bonn potential through the G matrix renormalization method [41] and included in the OXBASH package [42]. It is widely used to investigate Cd and In isotopes [43–45]. All two-body matrix elements of the jj45pna Hamiltonian are scaled by a factor of 0.93 to better reproduce the systematic spectroscopic properties of nuclei around $A = 90$. The predicted low-lying levels, shown in Fig. 3, are calculated in the $\pi1f_{5/2}$, $\pi2p_{3/2}$, $\pi2p_{1/2}$, and $\pi1g_{9/2}$ model space, marked as model space I. Besides the calculations based on model space I, we also performed calculations by allowing at most one neutron to be excited across the $N = 50$ shell, in order to predict the excitation energy related to $N = 50$ core excitation. The calculations show that the excitation energy of the lowest level involving one-neutron excitation across the $N = 50$ shell is above 4.4 MeV. All excited states below 4 MeV are predicted to originate from proton excitations within the $\pi1f_{5/2}2p1g_{9/2}$ shell, as shown in Fig. 3. The calculations give an overall good description of the experimentally known (2^+) to (8^+) yrast states with the $\pi1g_{9/2}^{-2}$ configuration. Moreover, four more states with $J^\pi = 5^-, 4^-, 0^+$,
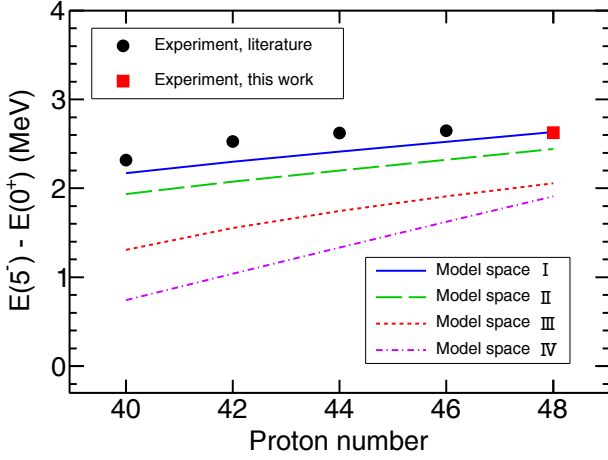
FIG. 4. Energy difference between the first 5^- and 0^+ ground states in $N = 50$ isotones. Data are taken from Refs. [20, 21, 28, 29] (black filled circles) and the present work (red filled square). The shell model calculations are performed using four different model spaces. See text for details.

and 3^- below 4 MeV are predicted. The first two states are the members of the $\pi 1 g_{9/2}^{-1} 2 p_{1/2}^{-1}$ doublet, the third one arises from the $\pi 2 p_{1/2}^{-2}$ configuration, and the fourth one has a configuration of $\pi 1 g_{9/2}^{-1} 2 p_{3/2}^{-1}$. The present calculations show that the position of the predicted 5^- state at 2635 keV is in good agreement with the newly observed state at 2627(12) keV, and the spin-parity of 5^- is well among the experimentally restricted candidates. Thus, the observed 2627(12)-keV state is suggested to be 5^- based on the $\pi 1 g_{9/2}^{-1} 2 p_{1/2}^{-1}$ configuration.

In fact, in the lighter $N = 50$ isotones ^{96}Pd, ^{94}Ru, ^{92}Mo, and ^{90}Zr, a 5^- state in each nucleus has been observed at similar excitation energy with the presently observed (5^-) state in ^{98}Cd, as displayed in Fig. 4. The continuation of a smooth trend of the 5^- state energies along the $N = 50$ isotones support the configuration assignment for the 5^- state in ^{98}Cd. For the decay pattern of the 5^- states in ^{96}Pd [21] and ^{94}Ru [25], besides the main decay path to the 4^+ states, a decay branch to the 6^+ states has been observed. The existence of the $5^- \rightarrow 6^+$ transition in the neighboring $N = 50$ isotones adds further confidence for the suggested assignment of the observed 346(8)-keV transition as decaying from the 5^- to 6^+ states in ^{98}Cd. In addition, the half-lives of the 5^- states in the ^{94}Ru and ^{92}Mo isotones have been measured to be 510(50) ps [20] and 1.55(4) ns [46], respectively. The deduced transition probabilities $B(E1)$ for the $5^- \rightarrow 4^+$ transitions in ^{94}Ru and ^{92}Mo are $7(1) \times 10^{-6}$ and $19.0(5) \times 10^{-6}$ e^2fm^2, respectively. The derived $B(E1)$ value for ^{98}Cd using the (5^-) state half-life obtained in this work is $18(5) \times 10^{-6}$ e^2fm^2. This strength is comparable to that observed in lighter isotones [20, 46].

To gain insights into the feature of the 5^- states along the $N = 50$ isotones, shell model calculations with differ-

ent model spaces are performed, as shown in Fig. 4. In addition to model space I, three other model spaces are used for comparison. For model space II, the $\pi 1 f_{5/2}$ orbital is omitted in comparison with model space I. Model space III is even smaller, as both the $\pi 1 f_{5/2}$ and $\pi 2 p_{3/2}$ orbitals are frozen as being fully occupied. Model space IV has the same orbitals as model space III, but at most one proton is allowed to be excited from the $\pi 2 p_{1/2}$ orbital. It can be seen in Fig. 4 that, when model space I is considered in the calculations, the experimental results of the 5^- excitation energies in the $N = 50$ isotones can be well reproduced by the theory. In the case of model space II, the calculated results slightly underestimate the experimental data. For model space III, the calculations exhibit obvious discrepancies with the data. Furthermore, the calculations with model space IV provide a rather poor description of the data especially for lower mass $N = 50$ isotones.

The calculations using model space I show that the $\pi 1 g_{9/2}^{-n} 2 p_{1/2}^{-1}$ ($n = 1, 3, 5, 7,$ and 9) components for the 5^- states in the $N = 50$ isotones ^{98}Cd, ^{96}Pd, ^{94}Ru, ^{92}Mo, and ^{90}Zr are 95.75%, 87.95%, 81.33%, 76.66%, and 75.14%, respectively. Although the $\pi 1 g_{9/2}^{-1} 2 p_{1/2}^{-1}$ configuration is the dominant component in all these five $N = 50$ isotones, the model space III (consisting of only the $\pi 2 p_{1/2}$ and $\pi 1 g_{9/2}$ orbitals) is insufficient to obtain a good agreement with the experimental 5^- excitation energies in the $N = 50$ isotones. This is mainly because the configuration components for the ground states are not pure. The calculations show that the $\pi 1 g_{9/2}^{-n}$ ($n = 2, 4, 6, 8,$ and 10) components for the ground states in ^{98}Cd, ^{96}Pd, ^{94}Ru, ^{92}Mo, and ^{90}Zr are only 83.20%, 67.56%, 53.18%, 39.58%, and 25.26%, respectively. The calculations also show that the proton excitations from the $\pi 2 p_{1/2}$ and $\pi 2 p_{3/2}$ orbitals to the $\pi 1 g_{9/2}$ orbital are important for the ground states. The missing $\pi 2 p_{3/2}$ orbital in model space III has reduced a large amount of correlation energy and raises the ground state energy, resulting in the disagreement between the calculated and experimental 5^- excitation energies. Therefore, a model space consisting of the $\pi 2 p_{3/2}$ orbital below the $Z = 38$ subshell, as well as the $\pi 2 p_{1/2}$ and $\pi 1 g_{9/2}$ orbitals is necessary to obtain a good agreement with the experimental 5^- data in the $N = 50$ isotones.

It is interesting to note that the first 8^+ state in the $N = 50$ isotones is predicted to have relatively pure $\pi 1 g_{9/2}^{-n}$ components as compared to the ground states. The calculations show that the $\pi 1 g_{9/2}^{-n}$ ($n = 2, 4, 6,$ and 8) components for the ground states in ^{98}Cd, ^{96}Pd, ^{94}Ru, and ^{92}Mo are 100%, 83.59%, 68.09%, and 52.41%, respectively. Thus, it is expected that the calculated energy difference between the 5^- and 8^+ states in the $N = 50$ isotones may not be strongly dependent on the model space. As shown in Fig. 5, the calculations using different model spaces give similar results and the experimental data are well reproduced by all calculations.
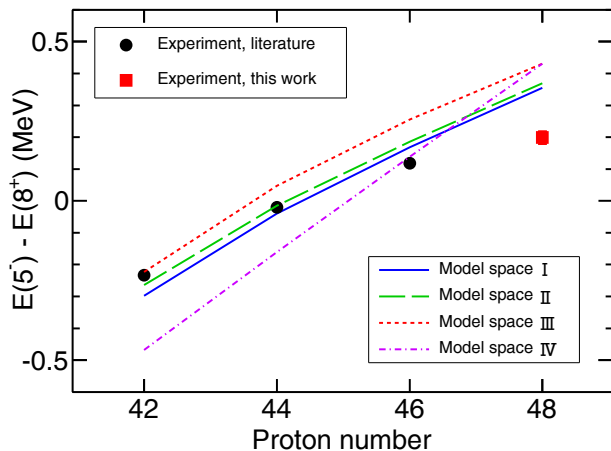
FIG. 5. The same as Fig. 4, but for the energy difference between the first 5^- and first 8^+ states in $N = 50$ isotones.

V. SUMMARY

In the present work, excited states in the proton-rich isotope ^{98}Cd have been populated via the two-nucleon removal reaction (^{100}In,^{98}Cd$+\gamma$). Four peaks were observed using the DALI2$^+$ γ-detection array, of which two peaks are observed for the first time. Based on γ-γ coincidence analysis, a new level at 2627(12) keV is placed in the level scheme of ^{98}Cd. The spin-parity of the identified state is tentatively assigned as 5^- based on the systematics of low-lying structures in proton-rich $N = 50$ isotones and shell-model predictions. The nature of

the (5^-) state is suggested to arise from a $\pi 1g_{9/2}^{-1} 2p_{1/2}^{-1}$ configuration. To understand the feature of the 5^- state energies in $N = 50$ isotones, shell model calculations with different model spaces are performed. The calculations show that, to reproduce the experimental data, the effect of the proton excitations from the $\pi 2p_{3/2}$ orbital should be taken into account for describing the 0^+ ground states.

[1] T. Faestermann, M. Górska, and H. Grawe, Prog. Part. Nucl. Phys. **69**, 85 (2013).
[2] T. D. Morris, J. Simonis, S. R. Stroberg, C. Stumpf, G. Hagen, J. D. Holt, G. R. Jansen, T. Papenbrock, R. Roth, and A. Schwenk, Phys. Rev. Lett. **120**, 152503 (2018).
[3] M. Siciliano *et al.*, Phys. Lett. B. **806**, 135474 (2020).
[4] Tomoaki Togashi *et al.*, Phys. Rev. Lett. **121**, 062501 (2018).
[5] R. Kumar *et al.*, Phys. Rev. C **96**, 054318 (2017).
[6] A. Corsi *et al.*, Phys. Lett. B. **743**, 451 (2015).
[7] G. Guastalla *et al.*, Phys. Rev. Lett. **110**, 172501 (2013).
[8] A. Banu *et al.*, Phys. Rev. C **72**, 061305 (2005).
[9] B. Cederwall *et al.*, Nature **469**, 68 (2011).
[10] B. S. Nara Singh *et al.*, Phys. Rev. Lett. **107**, 172502 (2011).
[11] P. J. Davies *et al.*, Phys. Rev. C **99**, 021302(R) (2019).
[12] C. Qi *et al.*, Phys. Rev. C **84**, 021301 (2011).
[13] S. Zerguine and P. Van Isacker, Phys. Rev. C **83**, 064314 (2011).
[14] S. Frauendorf and A. O. Macchiavelli, Prog. Part. Nucl. Phys. **78**, 24 (2014).
[15] J. Park *et al.*, Phys. Rev. C **96**, 044311 (2017).
[16] G. Häfner *et al.*, Phys. Rev. C **100**, 024302 (2019).
[17] M. Górska *et al.*, Phys. Rev. Lett. **79**, 2415 (1997).
[18] A. Blazhev *et al.*, J. Phys: Conf. Ser. **205**, 012035 (2010).

[19] A. Blazhev *et al.*, Phys. Rev. C **69**, 064304 (2004).
[20] A. Jungclaus *et al.*, Phys. Rev. C **60**, 014309 (1999).
[21] M. Palacz *et al.*, Phys. Rev. C **86**, 014318 (2012).
[22] M. Lipoglavšek *et al.*, Phys. Rev. C **72**, 061304(R) (2005).
[23] F. Ghazi Moradi *et al.*, Phys. Rev. C **89**, 014301 (2014).
[24] A. Ertoprak *et al.*, Eur. Phys. J. A **54**, 145 (2018).
[25] H. A. Roth *et al.*, Phys. Rev. C **50**, 1330 (1994).
[26] H. Mach *et al.*, Phys. Rev. C **95**, 014313 (2017).
[27] Christine Hornung *et al.*, Phys. Lett. B. **802**, 135200 (2020).
[28] T. Fukuchi *et al.*, Eur. Phys. J. A **24**, 249 (2005).
[29] E. K. Warburton, *et al.*, Phys. Rev. C **31**, 1184 (1985).
[30] Matjaž Vencelj *et al.*, Phys. Scr. **T125**, 222 (2006).
[31] L. Coraggio *et al.*, J. Phys. G: Nucl. Part. Phys. 26, 1697 (2000).
[32] J. Blomqvist and L. Rydström, Phys. Scr. **31**, 31 (1985).
[33] M. Honma *et al.*, Phys. Rev. C **80**, 064323 (2009).
[34] T. Kubo *et al.*, Prog. Theor. Exp. Phys. **2012**, 03C003 (2012).
[35] N. Fukuda *et al.*, Nucl. Instrum. Methods Phys. Res., Sect. B **317**, 323 (2013).
[36] S. Takeuchi *et al.*, Nucl. Instrum. Methods Phys. Res., Sect. A **763**, 596 (2014).
[37] I. Murray *et al.*, RIKEN Accel. Prog. Rep. **51**, 158 (2018).

[38] S. Agostinelli *et al.*, Nucl. Instrum. Methods Phys. Res., Sect. A **506**, 250 (2003).

[39] J. Allison *et al.*, Nucl. Instrum. Methods Phys. Res., Sect. A **835**, 186 (2016).

[40] N. Shimizu, T. Mizusaki, Y. Utsuno, and Y. Tsunoda, Computer Physics Communications **244**, 372, (2019).

[41] M. Hjorth-Jensen, T.T.S. Kuo, and E. Osnes, Phys. Rep. **261**, 125, (1995).

[42] B.A. Brown, A. Etchegoyan, and W.D.M. Rae, MSU Cyclotron Laboratory Report No. 524, (1986).

[43] M. Haaranen, P.C. Srivastava, and J. Suhonen, Phys. Rev. C **93**, 034308 (2016).

[44] M. Rejmund *et al.*, Phys. Lett. B **753**, 86 (2016).

[45] C. X. Yuan *et al.*, Phys. Lett. B **762**, 237 (2016).

[46] S. Cochavi, J. M. McDonald, and D. B. Fossan, Phys. Rev. C **3**, 1352 (1971).